Georisk
Vol. 2, No. 2, June 2008, 113–121

Reliability of passive earth pressure

D.V. Griffiths[a]*, Gordon A. Fenton[b] and Heidi R. Ziemann[a]

[a]*Division of Engineering, Colorado School of Mines, Golden Colorado, USA;* [b]*Department of Engineering Mathematics, Dalhousie University, Halifax, Nova Scotia, Canada*

(Received 4 December 2007; final version received 2 May 2008)

Passive earth pressure calculations in geotechnical analysis are usually performed with the aid of the Rankine or Coulomb theories of earth pressure based on uniform soil properties. These traditional earth pressure theories assume that the soil is uniform. The fact that soils are spatially variable leads to two potential problems in design: do sampled soil properties adequately reflect the effective properties of the entire soil mass and does spatial variability in soil properties lead to passive earth pressures that are significantly different from those predicted using traditional theories? This paper combines non-linear finite element analysis with random field simulation to investigate these two questions. The specific case investigated is a two-dimensional frictionless passive wall with a cohesionless drained soil mass. The wall is designed against sliding using Rankine's earth pressure theory. The unit weight is assumed to be constant throughout the soil mass and the design friction angle is obtained by sampling the simulated random soil field. For a single sample, the friction angle is used as an effective soil property in the Rankine model. For two samples, an average of the sampled friction angles is used. Failure is defined as occurring when the Rankine predicted passive resistance acting on the wall, modified by a factor of safety, is greater than that computed by the random finite element method. Using Monte Carlo simulation, the probability of failure of the traditional design approach is assessed as a function of the factor of safety using and the spatial variability of the soil.

Keywords: passive pressure; probabilistic analysis; finite elements; design; random fields

Introduction

Passive earth pressure calculations in geotechnical analysis are usually performed with the aid of the Rankine or Coulomb theories of earth pressure based on uniform soil properties. This paper compares the earth pressure predicted by Rankine's theory with those obtained using a finite element analysis in which the soil is assumed to be spatially random. For design purposes, the passive earth pressure computed this way will be reduced by a factor of safety. The specific case of a two-dimensional cohesionless drained soil mass with a horizontal upper surface retained by a vertical, frictionless, rigid wall is examined. The property of interest for a cohesionless soil is the friction angle. The wall is assumed to be able to translate toward the retained soil mass a sufficient distance to mobilise the passive resistance of the soil.

The traditional theory of lateral passive earth pressures is derived from equations of equilibrium along an assumed planar failure surface passing through the soil mass as shown in Figure 1.

For the retaining problem considered and a constant friction angle, Rankine proposed the passive earth pressure coefficient to be

$$K_p = \tan^2\left(45 + \frac{\phi'}{2}\right). \tag{1}$$

The soil's drained friction angle is ϕ'. The total lateral passive earth force acting on a wall of height H, at height $H/3$, is given by

$$P_p = \frac{1}{2}\gamma H^2 K_p. \tag{2}$$

The calculation of the lateral design load on a retaining wall requires an estimate of the friction angle, ϕ', and the unit weight, γ, and then the application of Equations (1) and (2). To include a margin of safety, the value of P_p is usually adjusted by dividing by a factor of safety, F.

Traditional theory may be used to model spatial variation provided the spatially random soil can be represented by an equivalent uniform soil, which is assigned an 'effective' property. It has been shown for several geotechnical problems that the effective soil property can be based on an appropriate average, e.g. geometric, of the random soil property (Griffiths and Fenton 2003).

In practice, the values of ϕ' and γ used in (1) and (2) are obtained through a site investigation. The spatial variability of the soil could be characterised by

*D.V. Griffiths. Email: Vgriffit@mines.edu

ISSN 1749-9518 print/ISSN 1749-9526 online

DOI: 10.1080/17499510802178640
http://www.informaworld.com

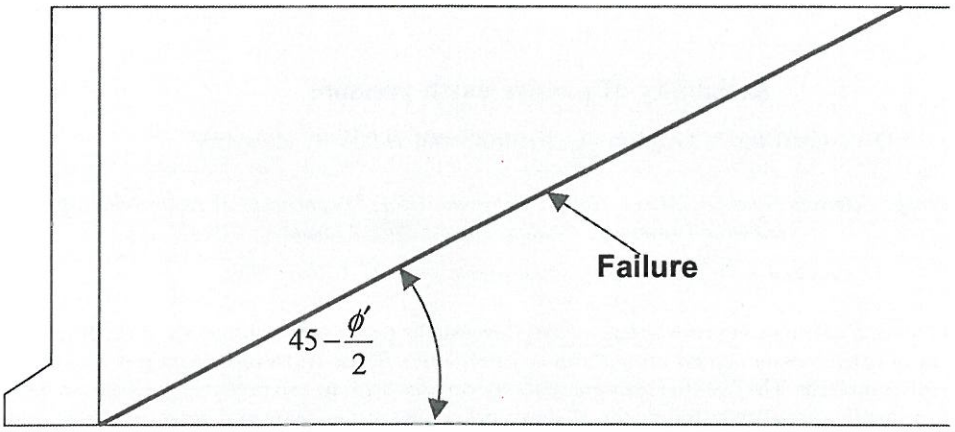

Figure 1. Classical passive Rankine failure plane.

a thorough site investigation and the effective soil property determined using random field theory and simulation results. However, it is not practical to conduct a site investigation that would sufficiently characterise the soil. It is more common for the geotechnical engineer to base the design on a single estimate of the friction angle. In this case, the accuracy of the prediction arising from (1) and (2) depends on how well the sampled value approximates the effective value.

This paper attempts to address the following questions:

a. Do sampled soil properties adequately reflect the effective properties of the entire soil mass?
b. Does spatial variability in soil properties lead to passive earth pressures that are significantly different from those predicted using traditional equations, such as Rankine's?

Figure 2 shows a displacement plot of what a typical soil might look like once the wall has moved enough to mobilise the passive soil behavior. The passive wall considered in this study is modeled by translating the top 41 nodes elements on the upper left side of the mesh uniformly horizontally and in the direction of the soil mass. This translation is performed incrementally, and models a rigid, smooth wall with no rotation. In our analyses, we are not modeling the wall explicitly, but simply incrementing the horizontal component of displacement of the nodes next to the 'wall'. We are not restraining the vertical components of displacement at these nodes however, so they are free to move. In Figure 2, we have assumed that the 'wall' moves with the nodes so in the passive case, this typically means a tendency for the 'wall' to move upwards as the soil deforms. The soil's spatially random friction angle is shown qualitatively using a grayscale representation of $\ln(\tan\phi)$, where light areas correspond to lower friction angles.

The wall is on the left-hand face, and the deformed mesh plots of Figure 2 is obtained using the random finite element method (RFEM) with

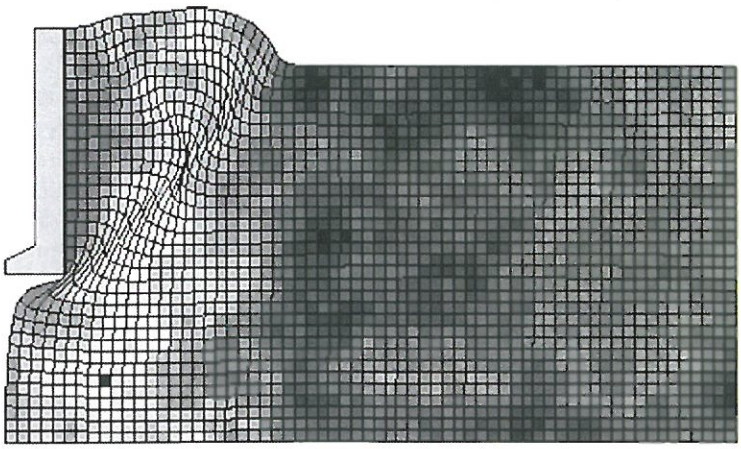

Figure 2. Passive earth displacement for a typical soil friction angle realisation ($\theta/H=0.5$ and $\sigma/\mu=0.1$).

eight-node square elements and an elastic perfectly plastic constitutive model (Griffiths and Fenton 2001). The wall is gradually moved toward the soil mass until plastic failure of the soil occurs, and the deformed mesh at failure is then plotted. Figure 2 shows a more complex failure pattern than that assumed using traditional theories such as Rankine's. The failure surface forms at regions of a lower friction angle and follows a path not defined by traditional theory but characterised by regions of lower strength. The formation of a failure surface can be viewed as the mechanism by which lateral loads stabilise to a constant value with increasing wall displacement.

Additionally, Figure 2 also shows the importance of the location of the sampled soil property. A soil sample taken at the midpoint of the soil mass shown in Figure 2 would result in a higher friction angle estimate than the friction angle seen near the failure region. In this case, the resulting predicted lateral passive load based on Rankine's theory would be more than 1.8 times that predicted using the RFEM, so that the wall designed using the soil sample would be unconservative.

The random finite element model

The soil mass is discretised into a mesh that consists of 64 eight-noded square elements in the horizontal direction by 32 elements in the vertical direction. Each element has a side length of 0.05. The wall extends to a depth of 20 elements or a unit length along the left face. (Note: units are not used herein as the results are applicable to any consistent set of length and force units.)

The boundary conditions are such that the right side of the mesh allows vertical but not horizontal movement, the base of the mesh is fully restrained. The top and left sides of the mesh are unrestrained, with the exception of the nodes adjacent to the 'wall', which have fixed horizontal components of displacement. The vertical components of these displaced nodes are free to move up, as passive conditions are mobilised, thereby modeling a perfectly smooth condition. Smooth conditions are assumed on account of their simplicity and conservatism for passive earth pressure computations.

The finite element earth pressure analysis uses an elastic-perfectly Mohr–Coulomb constitutive model with stress redistribution achieved iteratively using a reduced integration elasto-viscoplastic algorithm similar to that described and validated for uniform soils by Smith and Griffiths (2004). The analyses use reduced integration in both the stiffness and stress distribution phases of the algorithm.

The initial stress conditions in the mesh prior to translation of the nodes are that the vertical stresses equal the weight of the overburden, or

$$\sigma_v = \gamma z, \tag{3}$$

where γ is the unit weight of the soil and z is the depth to the Gauss points of the element, positive down. The unit weight, γ, is assumed to be constant. The variability of γ is not considered due to the fact that its range of variability is small relative to the friction angle (e.g. Kulhway and Phoon 1999). The initial horizontal stresses are defined by the coefficient of earth pressure at rest, K_0, given by Jaky's (1944) formula in which

$$K_0 = 1 - \sin \phi'. \tag{4}$$

The study will assume that $\tan \phi'$ is a log-normally distributed field: hence K_0 will also be a random field dependent on the value of ϕ' within each element adjacent to the wall. The initial horizontal stress against the wall 'at rest' will therefore be randomly distributed about a linearly increasing trend line with the equation $\mu_{\sigma_h} = \mu_{K_0} \gamma z$ where μ_{K_0} is the mean earth pressure coefficient at rest based on Jaky's formula with the mean friction angle. The soil is assumed to be cohesionless as is common for backfill materials.

This initial stress state is not in equilibrium because the horizontal stresses in adjacent elements are unequal; however, this would also be the case with the vertical stresses between adjacent elements if we had elected to include a random unit weight γ. This initial lack of equilibrium is not an issue, because it is quickly corrected as soon as the wall starts to move and the soil starts to yield by the nonlinear viscoplastic algorithm as explained in the next paragraph.

Following incremental displacement of the nodes, the viscoplastic algorithm monitors the stresses in all the elements (at the Gauss points) and compares them with the strength of the element based on Mohr–Coulomb's failure criterion. If the failure criterion is not violated, the element is assumed to remain elastic; however, if the criterion is violated, stress redistribution is initiated by the viscoplastic algorithm. The process is inherently iterative, and convergence is achieved when all stresses within the mesh satisfy both the failure criterion and equilibrium within quite a tight tolerance.

At convergence following each increment of displacement, the mobilised passive reaction force on the wall is computed by integrating the stress in the elements attached to the displaced nodes. The finite element analysis is terminated when the passive reaction force flattens out and reaches a maximum value. The role of K_0 on the ultimate passive resistance in a probabilistic context may be a topic

for further research; however, classical earth pressure theory indicates that it has no influence.

The soil property of interest in the cohesionless soil being studied is the tangent of the friction angle, $\tan \phi'(\underset{\sim}{x})$, where $\underset{\sim}{x}$ is the spatial position. The tangent of the friction angle is assumed to be a spatially random field. The finite element model used in this study includes the unit weight, γ, taken to be 20, the soil dilation angle, taken to be zero, Poisson's ratio, taken to be 0.3 and Young's modulus, taken to be 1×10^5. These properties are assumed to be spatially constant.

The spatially random property, $\tan \phi'$, is characterised by a mean (μ), a standard deviation (σ), and a correlation length (θ). $\tan \phi'$ varies from 0 to infinity and can be defined by a log-normal distribution. The distribution assumed in this paper is that the friction angle field will be represented by the log-normally distributed $\tan \phi'$ field.

The correlation function for the $\ln(\tan \phi')$ fields is assumed to be Markovian:

$$\rho(\tau) = \exp\left(\frac{-2|\underset{\sim}{\tau}|}{\theta}\right), \tag{5}$$

where θ is the correlation length beyond which two points in the field are largely uncorrelated, $\underset{\sim}{\tau}$ is the vector between the two points, and $|\underset{\sim}{\tau}|$ is its absolute length.

A normal random field, $G_1(\underset{\sim}{x})$, is simulated by the local average subdivision (LAS) method (Fenton and Vanmarke 1990), using the correlation structure given by Equation (5). The field is then transformed to the target field through the relationship

$$\tan \phi'(\underset{\sim}{x}) = \exp(\mu_{\ln \tan \phi'} + \sigma_{\ln \tan \phi'} G_1(\underset{\sim}{x})), \tag{6}$$

where μ and σ are the mean and standard deviation of subscripted value, obtained using the following transformations:

$$\sigma^2_{\ln \tan \phi'} = \ln(1 + V^2_{\tan \phi'}) \tag{7}$$

$$\mu_{\ln \tan \phi'} = \ln(\mu_{\tan \phi'}) - \frac{1}{2}\sigma_{\ln \tan \phi'}, \tag{8}$$

and $V_{\tan \phi'} = \sigma_{\tan \phi'}/\mu_{\tan \phi'}$ is the coefficient of variation of $\tan \phi'$.

Once realisations of the soil have been produced using LAS and the above transformations, the properties can be mapped to the elements and the soil mass analysed by the finite element method. Repeating this analysis using Monte-Carlo simulation generates a series of computed responses which can be used to estimate the distribution of the responses.

Passive earth pressure design reliability

Passive earth pressures are typically computed by estimating the relevant soil properties and predicting the lateral load through, for example, Equation (2). The reliability of the design depends on the relationship between the predicted and actual lateral loads. Defining the design wall resistance, R as

$$R = \frac{P_p}{F}, \tag{9}$$

where F is a factor of safety and P_p is the predicted passive lateral earth load, then 'design failure' will occur if the true passive resistance falls below the factored design value P_p/F. The true passive lateral resistance will differ from that predicted because of errors in the estimation of soil properties and due to spatial variation in the true soil mass. The probability of failure of the retaining system will be defined as the probability that the true lateral load, P_t, is less than the factored resistance:

$$p_f = P[P_t < R] = P\left[P_t < \frac{P_p}{F}\right], \tag{10}$$

where P_t is assumed to be the load computed in the finite element analysis for each soil realisation.

In this study, the predicted lateral load P_p depends on an estimate of the friction angle, ϕ' as might be obtained from a single borehole sample performed as part of a rather rudimentary site investigation. In this paper, the friction angle will be estimated using a 'virtual sample' which will be the value of the friction angle generated at a specific location within the random field. In this study, the location of the single sample will be at the average depth of the wall ($H/2$) and at variety of distances away from the wall as shown in Table 1.

A friction angle is obtained from each random field realisation as

$$\hat{\phi}' = \tan^{-1}\{\tan[\phi'(\underset{\sim}{x}_s)]\} \tag{11}$$

which is then used to compute the predicted passive force

Table 1. Location of virtual sample point $\underset{\sim}{x}_s$ in the study.

Virtual sample point no.	Horizontal distance from wall	Vertical distance from soil surface
1	H/4	H/2
2	H/2	H/2
3	H	H/2
4	2H	H/2

Table 2. Parameters varied in study while holding the retained soil dimension H, and soil properties $\mu_{\tan\phi'} = \tan 30°$, $\gamma = 20$, $E = 1 \times 10^5$, $\nu = 0.3$ constant.

Parameter	Values considered
σ/μ	0.02, 0.05, 0.1, 0.2, 0.3, 0.5
θ/H	0.025, 0.05, 0.1, 0.2, 0.5, 1.0, 2.0, 5.0

$$P_p = \frac{1}{2}\gamma H^2 \tan^2\left(45 + \frac{\hat{\phi}'}{2}\right). \quad (12)$$

The predicted value from Equation (12) at each realisation is then compared with the limiting passive resistance computed by the random finite element method given by R from Equation (10).

Table 2 lists the statistical parameters varied in this study. For each parameter set considered in Table 2, the factor of safety, F, has been varied in the range 1.1–1.5 (e.g. Duncan and Mokwa 2001).

The correlation length, θ, normalised in Table 1, governs the degree of spatial variability in the soil. Figure 3 shows the influence of a small correlation length on the random field. The field appears rough and the element properties vary rapidly from one point to another.

Figure 4 shows the influence of a large correlation length on the random field. The field appears smooth and the element properties vary gradually.

It has been shown (Fenton *et al.* 2005) that for large values of θ/H the soil properties estimated by the virtual sample will be more representative of the overall soil mass and therefore more accurately define the effective property. The reduction in spatial variability means that values produced by traditional theories are more accurate with regard to actual behavior. Therefore, fewer failures are expected (where the true lateral load, P_t, is less than the factored resistance, P_P) at higher values of θ/H. For this case, a reduced factor of safety can be used and a single virtual sample will be adequate to estimate the effective soil properties. For intermediate values of θ/H, the sampled soil properties may vary greatly based on location. More failures are expected and a higher factor of safety will be required if only one virtual sample point is used to characterise the soil mass. Additional sample points will reduce the failures and factor of safety requirements. For extremely small values of θ/H, local averaging effects begin to be dominant and the soil mass modeled by the random finite element method will behave like a uniform soil and can be accurately predicted by traditional theories with the soil property set to the median.

For this reason, the maximum probability of failure of the design is expected to occur when the correlation length is at some intermediate value for the case of one virtual sample point. Additionally, the inclusion of additional sample points should not greatly influence the probability of failure of random fields with large θ/H values. The influence on random fields with smaller values of θ/H should be evident. The next section will provide evidence supporting the above.

Monte Carlo results based on virtual sampling

Figures 3 and 4 showed the migration of the failure surface to areas of lower friction angles. The tendency of the failure surface to 'seek out' the weaker path means that, in general, the lateral wall load will be different from the load predicted assuming uniform soil properties and traditional theories such as Rankine's. Figures 5 and 6 show the estimated probability of failure, p_f, that the true lateral passive load will be less than the factored predicted design load (see Equation (10)) for a correlation length ($\theta/H = 1.0$) and for various coefficients of variation in the friction angle. The estimates are obtained by

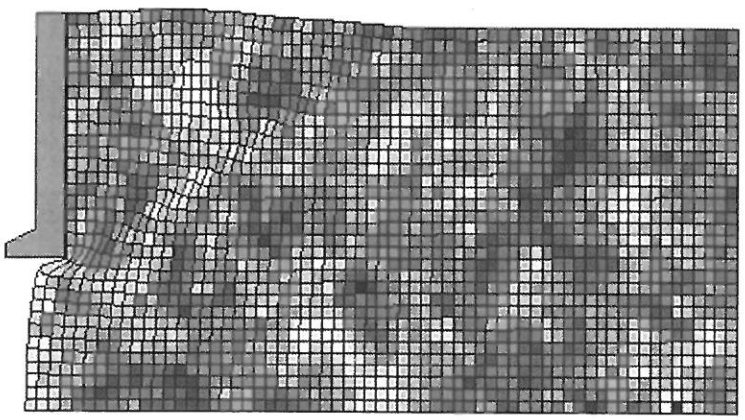

Figure 3. Passive earth displacement for a typical soil friction angle realisation ($\theta/H = 0.2$ and $\sigma/\mu = 0.1$).

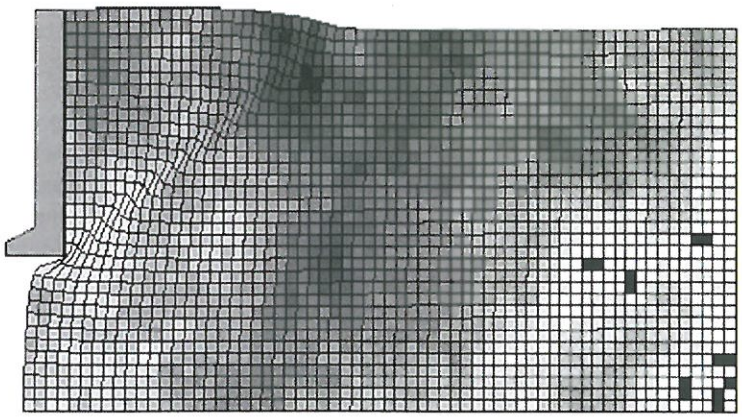

Figure 4. Passive earth displacement for a typical soil friction angle realisation ($\theta/H = 5.0$ and $\sigma/\mu = 0.1$).

counting the number of failures encountered in the simulation and dividing by the total number of realisations, n ($n = 1000$). The standard error (one standard deviation) associated with the estimate is $\sqrt{p_f(1-p_f)/n}$, which is about 1% when $p_f = 20$ and 0.3% when $p_f = 1.0\%$. Figure 5 shows the estimated probability of failure, p_f, that the true lateral passive load will be less than the factored predicted design load based on a single virtual sample point located as defined by virtual sample point 1 (see Table 1). Figure 6 shows the estimated probability of failure, p_f, that the true lateral passive load will be less than the factored predicted design load based on a single virtual sample point located as defined by virtual sample point 2 (see Table 1) $p_f = P[P_t < P_p/F]$.

As expected, the probability of failure increases as the soil becomes increasingly variable. Figure 5 can be used to determine a target probability of failure. For example, from Figure 5, with $V = 0.2$, a factor of safety of approximately $F = 1.5$ would be required for $p_f < 2\%$.

The influence of the location of a single sample point is shown in Figures 6 and 7. For an intermediate value of $\theta/H = 1.0$ shown in Figure 6, a single sample point located at $2H$ away from the wall, $H/2$ deep with $V = 0.3$, and a factor of safety of 1.5 the probability of failure is about 12%. For the single sample point located at $H/2$, $H/2$, the probability of failure is about 7%.

For a large value of $\theta/H = 5.0$ shown in Figure 7, a single sample point located at ($2H$, $H/2$) with $V = 0.3$, and a factor of safety is 1.5 the probability of failure is 4.8%. For the single sample point located at ($H/2$, $H/2$), the probability of failure is 1.8%. Both Figures 6 and 7 point to an optimal location for a

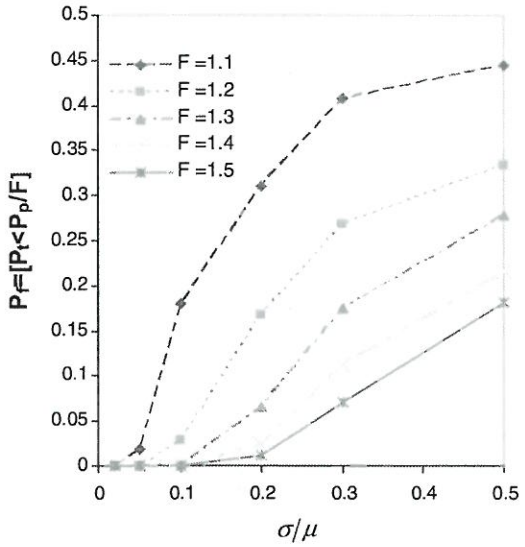

Figure 5. p_f, for $\theta/H = 1.0$, design load based on virtual sample point at (H/2, H/2).

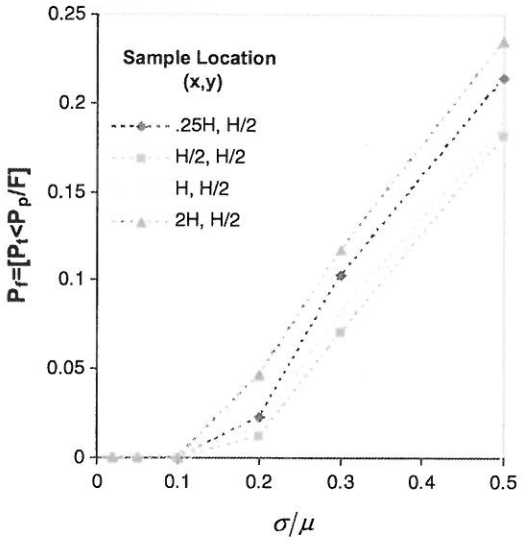

Figure 6. p_f, for $\theta/H=1.0$ ($F=1.5$).

single sample point located at a horizontal distance between mid height and the total height of the wall.

Recalling that one virtual sample point was used to characterise the soil, the required factor of safety should be reduced if two samples are taken as shown in Figure 8. From Figure 8, with $V=0.2$, a factor of safety of approximately $F=1.5$ gives a probability of failure that would approach 0.0%.

Figure 9 shows the estimated probability of failure, p_f, for $V=0.2$ against the correlation length, θ/H. Of interest is the fact that there is a maximum probability of failure associated with correlation lengths between $\theta/H=0.1$ to $\theta/H=1.0$. This worst case θ/H range is seen in all of the soil coefficients of variation considered. This observation can be used to define a conservative design case used for reliability analysis when additional information is not available.

Concluding remarks

On the basis of this simulation study, the following observations can be made:

1. The traditional approach to geotechnical design rarely takes account of soil property variations in a systematic way. In most cases analyses are performed with an equivalent or 'effective' property that represents some kind of 'average' value. This is followed by the application of a blanket Factor of Safety to

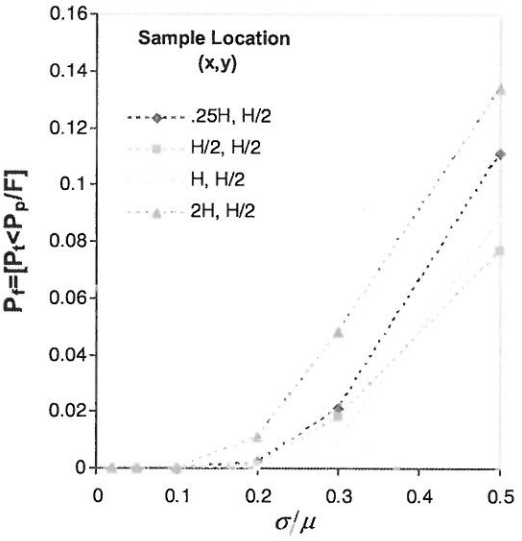

Figure 7. p_f, for $\theta/H=5.0$ ($F=1.5$).

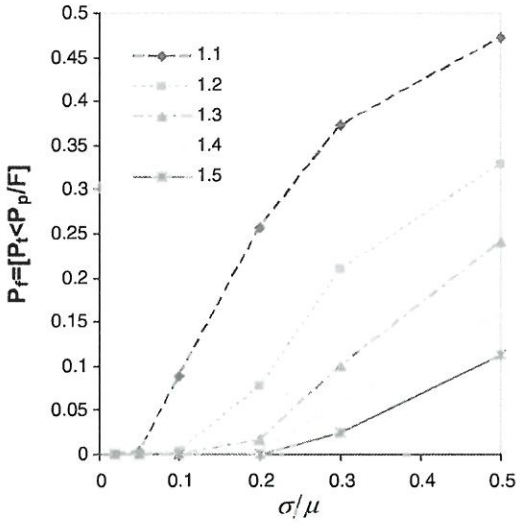

Figure 8. p_f, for $\theta/H = 1.0$, design load based on average value of virtual sample points at (H/2, H/2) and (H, H/2).

account for all sources of variability that were not considered directly.

2. The failure mode of the passive case forms at regions of a lower friction angle and follows a path not defined by traditional theory but characterised by regions of lower shear strength. The mechanism 'seeks out' the weakest path through the soil mass.
3. A single sample point located at a horizontal distance near to the height of the wall tends to provide a better estimate of the effective soil properties, producing a lower probability of failure independent of assumed scale of fluctuation.

   The inclusion of additional sample points to characterise the soil properties reduces the probability of failure.
4. Consistent with a number of classical geotechnical problems (e.g. differential settlement, bearing capacity, and active earth pressure), a worst-case scale of fluctuation exits for the passive earth pressure problem, which is near to the retaining wall height. Because of this observation, the scale of fluctuation does not

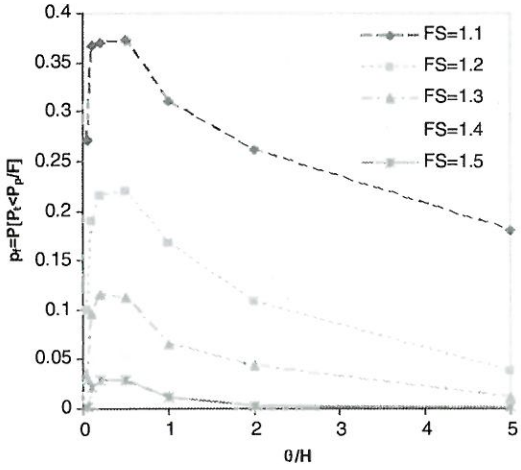

Figure 9. Estimated probability that true load is less than design load, p_f for $\sigma/\mu = 0.2$ and design load based on single sample at H/2, H/2.

need to be estimated; the worst-case scale of fluctuation can be used to generate a conservative design at a target reliability.

Notation

E	Young's modulus
F	factor of safety
$G(x)$	standard normal (Gaussian) random field
H	depth of retaining wall
K_p	passive earth pressure coefficient
K_0	coefficient of earth pressure at rest
n	number of realisations
p_f	probability of failure
P_p	passive lateral load predicted by Rankine
P_t	true lateral load approximated by RFEM
R	retaining wall resistance, P_p/F
V	coefficient of variation, σ/μ
$\underset{\sim}{x}$	spatial coordinate position
γ	unit weight
θ	correlation length
μ	random field mean
$\mu_{\tan \phi'}$	mean of tangent of drained friction angle
$\mu_{\ln \tan\phi'}$	mean of logarithm of tangent of drained friction angle
μ_{K_0}	mean of the earth pressure coefficient at rest
ν	Poisson's ratio
ρ	point-wise correlation between ln(tanϕ') random fields
σ	random field standard deviation
$\sigma_{\ln \tan \phi'}$	standard deviation of the logarithm of the tangent of the drained friction angle
σ'	effective stress
$\underset{\sim}{\tau}$	vector between two points in a random field
ϕ'	drained friction angle
$\hat{\phi}'$	estimated drained friction angle

Acknowledgements

The authors wish to acknowledge the support of NSF grant CMS-0408150 on 'Advanced probabilistic analysis of stability problems in geotechnical engineering'.

References

Duncan, J.M. and Mokwa, R.L., 2001. Passive earth pressure: Theories and tests. *ASCE: Journal of Geotechnical and Geoenvironmental Engineering*, 127 (3), 248–257.

Fenton, G.A. and Griffiths, D.V., 2003. Bearing capacity of spatially random c-ϕ soils. *Canadian Geotechnical Journal*, 40 (1), 54–65.

Fenton, G.A. and Vanmarcke, E.H., 1990. Simulation of random fields via local average subdivision. *ASCE: Journal of Engineering Mechanics*, 116 (8), 1733–1749.

Fenton, G.A., Griffiths, D.V., and Williams, M.B., 2005. Reliability of traditional retaining wall design. *Geotechnique*, 55 (1), 55–62.

Griffiths, D.V. and Fenton, G.A., 2001. Bearing capacity of spatially random soil: The undrained clay Prandtl problem revisited. *Geotechnique*, 51 (4), 351–359.

Jaky, J., 1948. Pressure in silos. *Proceedings of the Second International Conference on Soil Mechanics and Foundation Engineering*, 1, Rotterdam, The Netherlands, 103–107.

Kulhway, F.H. and Phoon, K., 1999. Characterization of geotechnical variability. *Canadian Geotechnical Journal*, 36, 612–624.

Smith, I. M. and Griffiths, D.V., 2004. *Programming the finite element method*. 4th ed. New York: John Wiley & Sons.